An Accuracy Evaluation of Unstructured Node-Centred Finite Volume Methods

Magnus Svard
Stanford University, Stanford, California

Jing Gong
Uppsala University, Uppsala, Sweden

Jan Nordstrom
The Swedish Defense Research Agency, Stockholm, Sweden and
Uppsala University, Uppsala, Sweden

April 2006

Since its founding, NASA has been dedicated to the advancement of aeronautics and space science. The NASA Scientific and Technical Information (STI) Program Office plays a key part in helping NASA maintain this important role.

The NASA STI Program Office is operated by Langley Research Center, the lead center for NASA's scientific and technical information. The NASA STI Program Office provides access to the NASA STI Database, the largest collection of aeronautical and space science STI in the world. The Program Office is also NASA's institutional mechanism for disseminating the results of its research and development activities. These results are published by NASA in the NASA STI Report Series, which includes the following report types:

- TECHNICAL PUBLICATION. Reports of completed research or a major significant phase of research that present the results of NASA programs and include extensive data or theoretical analysis. Includes compilations of significant scientific and technical data and information deemed to be of continuing reference value. NASA counterpart of peer-reviewed formal professional papers, but having less stringent limitations on manuscript length and extent of graphic presentations.

- TECHNICAL MEMORANDUM. Scientific and technical findings that are preliminary or of specialized interest, e.g., quick release reports, working papers, and bibliographies that contain minimal annotation. Does not contain extensive analysis.

- CONTRACTOR REPORT. Scientific and technical findings by NASA-sponsored contractors and grantees.

- CONFERENCE PUBLICATION. Collected papers from scientific and technical conferences, symposia, seminars, or other meetings sponsored or co-sponsored by NASA.

- SPECIAL PUBLICATION. Scientific, technical, or historical information from NASA programs, projects, and missions, often concerned with subjects having substantial public interest.

- TECHNICAL TRANSLATION. English-language translations of foreign scientific and technical material pertinent to NASA's mission.

Specialized services that complement the STI Program Office's diverse offerings include creating custom thesauri, building customized databases, organizing and publishing research results ... even providing videos.
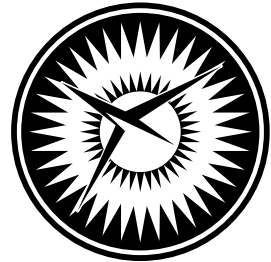
For more information about the NASA STI Program Office, see the following:

- Access the NASA STI Program Home Page at *http://www.sti.nasa.gov*

- E-mail your question via the Internet to help@sti.nasa.gov

- Fax your question to the NASA STI Help Desk at (301) 621-0134

- Phone the NASA STI Help Desk at (301) 621-0390

- Write to:
  NASA STI Help Desk
  NASA Center for AeroSpace Information
  7121 Standard Drive
  Hanover, MD 21076-1320

NASA/CR-2006-214293
NIA Report No. 2005-04

An Accuracy Evaluation of Unstructured Node-Centred Finite Volume Methods

Magnus Svard
Stanford University, Stanford, California

Jing Gong
Uppsala University, Uppsala, Sweden

Jan Nordstrom
The Swedish Defense Research Agency, Stockholm, Sweden and
Uppsala University, Uppsala, Sweden

Available from:

An Accuracy Evaluation of Unstructured Node-Centred Finite Volume Methods

Magnus Svärd,* Jing Gong†and Jan Nordström,‡

Abstract

Node-centred edge-based finite volume approximations are very common in computational fluid dynamics since they are assumed to run on structured, unstructured and even on mixed grids.

We analyse the accuracy properties of both first and second derivative approximations and conclude that these schemes can not be used on arbitrary grids as is often assumed. For the Euler equations first-order accuracy can be obtained if care is taken when constructing the grid. For the Navier-Stokes equations, the grid restrictions are so severe that these finite volume schemes have little advantage over structured finite difference schemes. Our theoretical results are verified through extensive computations.

1   Introduction

Finite volume approximations are widely used in computational fluid dynamics (CFD). There are several different variations of finite volume approximations and one of the more popular is the node-centred edge-based approximation. (See [1–13].) One reason for its popularity is the simple data structures associated with this scheme which make aerodynamic computations very efficient. Another is that it is assumed to run on grids made

---

*Center for Turbulence Research, Building 500, Stanford University, Stanford, CA 94305-3035, USA, e-mail: svard@stanford.edu

†Department of Information Technology, Uppsala University , Uppsala, Sweden.

‡Department of Computational Physics, Division of Systems Technology, The Swedish Defense Research Agency, SE-164 90 Stockholm, Sweden and Department of Information Technology, Uppsala University , Uppsala, Sweden.
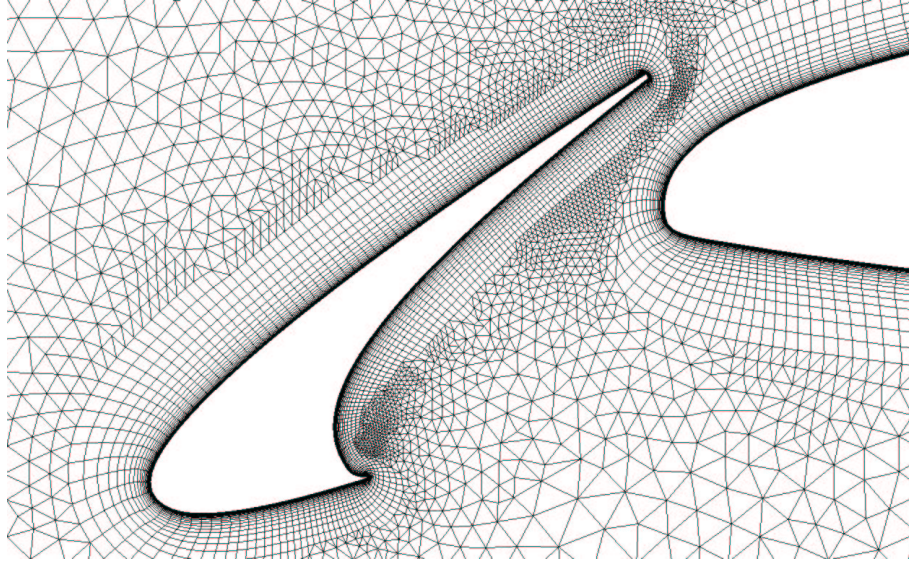
Figure 1: A typical CFD finite volume grid for a wing.

up of any type of elements, such as quadrilaterals or triangles in two space dimensions or tetrahedrons, prisms etc in three dimensions. Not only is the scheme assumed to yield at least first-order accuracy on all these element types but it is also assumed that a grid may mix element types. Such a grid is seen in Fig. 1. (See [14] and also [13, 15, 16] for more hybrid grids.) This property was called grid transparency in [1] and it is a crucial property since it greatly simplifies the task of grid generation.

In a sequence of previous articles [8, 9, 17], the present authors have investigated the accuracy and stability of the edge-based finite volume approximation for both hyperbolic and parabolic problems. In this paper we focus on accuracy questions for Cauchy problems. We review and extend the analysis of the previous papers to give a coherent view of the accuracy of the edge-based finite volume approximation.

Often, it is assumed that by only including the Laplacian part of the viscous terms, a good approximation for the Navier-Stokes equations is obtained and that makes it possible to construct a compact discretisation for the viscous terms.

We will consider the scalar advection-diffusion equation as a model for the Navier-Stokes equations,

$$u_t + au_x + bu_y = \epsilon(u_{xx} + v_{yy}). \tag{1}$$

This equation contains the most important terms appearing in the Navier-Stokes equations and if (1) is accurately approximated, the same is true for

the Navier-Stokes equations.

The contents of this report are divided as follows; in Section 2 we will present the edge-based finite volume approximations; then follow Section 3 and 4 containing accuracy studies for the Laplacian approximation and the advection equation respectively. Finally, conclusions are drawn in Section 5.

2 The Finite Volume Approximation

We begin by stressing that neither of the schemes derived below are due to the present authors but rather standard schemes used in CFD (c.f. [1]-[13],[17],[18]).

Following the derivation in [8], we begin with one advective term and consider equation (1) with $b = \epsilon = 0$. The finite volume approximation is derived from the weak form of the equation,

$$\iint_{V_i} u_t dx dy + a \iint_{V_i} u_x dx dy = 0. \tag{2}$$

Before we proceed to approximate (2) we introduce some notation. The discrete solution will be defined at a grid vertex (c.f Fig. 2). (That defines a node-centred scheme.) Let r_i denote a grid point and let V_i be an n-sided polygon with sides ds_{in}. V_i is defined as the volume inside the dual grid around r_i. The dual grid is in turn defined as the straight lines drawn between the centres of mass of the cells with r_i as a vertex and the midpoints of the edges from r_i, see Fig. 2. Further, ds_{in} is defined as the sum of the length of the "centre of mass-midpoint-centre of mass" lines passing over one edge (see Fig. 2). We will denote the measure of the volume V_i , although it is a slight abuse of notation since the volume itself is also denoted V_i.

Further, let $(u_N)_{in}$ denote the outward pointing derivative normal to ds_{in}. Let $r_{in} = |r_i - r_n|$. Finally, let N_i denote the set of indices of points being neighbours to r_i.
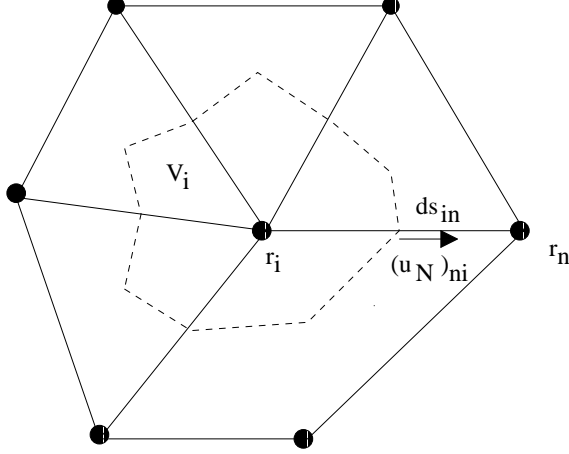
Figure 2: A generic 2D grid. Solid lines are the grid lines and dashed lines corresponds to the dual grid.

Now we return to equation (2). The integration is carried out over a dual volume of size V_i for point r_i (Fig. 2).

$$\iint_{V_i} u_t \, dx dy + a \oint_{\partial V_i} u \, dy = 0 \tag{3}$$

Along each ds_{in} we approximate the solution by $(u_n + u_i)/2$, where u_n and u_i are the discrete solution values at r_n and r_i. We obtain,

$$V_i(u_i)_t + a \sum_{n \in N_i} \frac{u_i + u_n}{2} \Delta y_n = 0, \tag{4}$$

where the sum ranges over all neighbours to u_i and Δy_n is the difference in y along ds_{in}. A similar approximation is obtained for the y-derivative.

On a rectangular grid with a smooth mapping to a Cartesian grid, the first derivative approximation in (4) can be proven second-order accurate using Taylor expansions. It is also possible to prove first-order accuracy on an unstructured triangular grid (see Appendix I). This is an upper bound of the error and on highly regular grids the error may even be second-order.

As mentioned in the introduction, a common approximative model for the viscous terms used in computations with the Navier-Stokes equations is to only include the Laplacian. Following the derivation in [9], assume that $a = b = 0$ and $\epsilon = 1$ in equation (1) and integrate over the domain V_i. We obtain,

$$\int_{V_i} u_t dv = \int_{\partial V_i} \frac{\partial u}{\partial N} ds, \tag{5}$$

4

where Gauss' theorem is used. N denotes the outward pointing unit normal vector such that $\frac{\partial u}{\partial N} = u_N = \nabla u \cdot N$. A straightforward approximation of (5) would be,

$$V_i(u_t)_i = \sum_{n \in N_i} (u_N)_{in} ds_{in}. \tag{6}$$

The normal derivative to ds_{in} $((u_N)_{in})$, is approximated by the central difference along that edge and we obtain for an interior point r_i,

$$V_i(u_t)_i = \sum_{n \in N_i} \frac{u_n - u_i}{r_{ni}} ds_{in}. \tag{7}$$

Using Taylor expansions this approximation can be shown second-order accurate on Cartesian grids.

3 Accuracy of Laplacian on unstructured grids

In [9] the approximation (7) of the Laplacian was studied and a stable implementation of the boundary conditions derived and several computations were made for the wave equation $u_{tt} = \Delta u$ in two space dimensions. A grid convergence study was made and the results are shown in Fig. 3 for a Cartesian mesh. Second-order accuracy is obtained in this case.
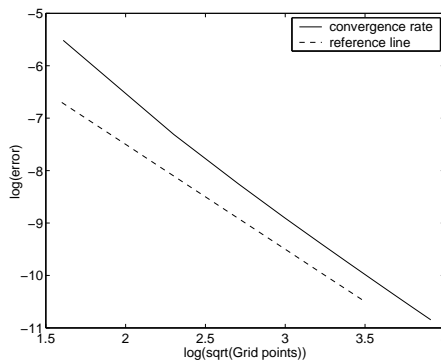

Figure 3: Grid convergence in l_2, for the wave equation on a Cartesian mesh. The dashed reference line represents second-order of accuracy.

Next, we tested the scheme on a triangulated Cartesian grid (see Fig. 4). As this kind of grid is refined, the convergence results are poor as seen in Fig. 4. The reason for the bad grid convergence will be analysed in the following subsection.
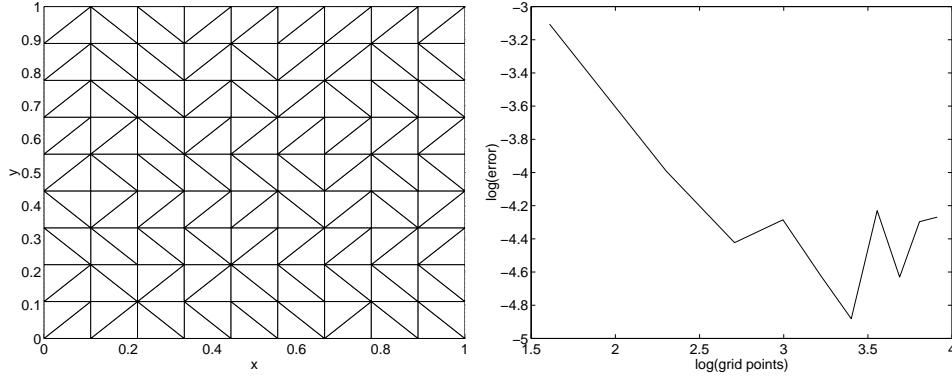
Figure 4: *Left:* A triangulated Cartesian mesh. *Right:* l_2-convergence on a triangulated Cartesian mesh.

Remark A triangulated Cartesian grid is not truly an unstructured grid. But it is a good model of an unstructured grid and if the scheme is inconsistent on such a grid it will not be consistent on an arbitrary unstructured grid.

3.1 Consistency Analysis

We will analyse consistency for the centre point of the grid in Fig. 5. The scheme (7) leads to,

$$V_1(u_1)_t = \sum_{i=2}^{7} \frac{u_i - u_1}{r_{i1}} ds_{i1}, \tag{8}$$

where $V_1 = h^2$ is the area inside the dashed line. By Taylor expansions we obtain for the edge r_{21}.

$$\frac{u_2 - u_1}{\sqrt{2}h} = \frac{u_1 + hu_x + hu_y + \frac{1}{2}(h^2 u_{xx} + 2h^2 u_{xy} + h^2 u_{yy}) - u_1 + \mathcal{O}(h^3)}{\sqrt{2}h},$$

where the derivatives are taken at point 1. A similar derivation for edge r_{51} leads to,

$$\frac{u_2 - u_1}{\sqrt{2}h} ds_{12} + \frac{u_5 - u_1}{\sqrt{2}h} ds_{15} = \frac{h^2 u_{xx} + 2h^2 u_{xy} + h^2 u_{yy} + \mathcal{O}(h^3)}{3}.$$

In the same manner we obtain for points edges r_{31}, r_{41}, r_{61} and r_{71}.

$$\frac{u_3 - u_1}{h} ds_{13} + \frac{u_6 - u_1}{h} ds_{16} = \frac{\sqrt{5}}{3}(h^2 u_{xx} + \mathcal{O}(h^3)),$$

$$\frac{u_7 - u_1}{h} ds_{17} + \frac{u_4 - u_1}{h} ds_{14} = \frac{\sqrt{5}}{3}(h^2 u_{yy} + \mathcal{O}(h^3)).$$

6

Summing up, using (8) and $V_1 = h^2$ yield,

$$(u_1)_t = \frac{1 + \sqrt{5}}{3}\Delta u + \frac{2}{3}u_{xy} + \mathcal{O}(h),$$

i.e. an $\mathcal{O}(1)$ error. This is stated in theorem 3.1.

Theorem 3.1 *On a general grid the approximation (7) of (1), with $a = b = 0$ and $\epsilon = 1$, is inconsistent.*
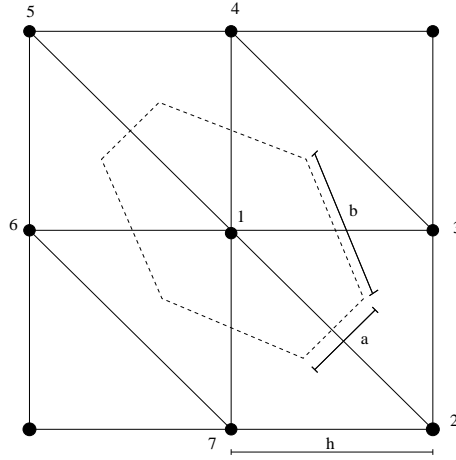

Figure 5: A triangular grid where the dual grid is the dashed line, $b = h\sqrt{5}/3$ and $a = h\sqrt{2}/3$.

The theorem does not imply inconsistency on all grids. It is easily seen in the above analysis that if the scheme consists of equilateral polygons, consistency is recovered. This is verified with computations on a grid with equilateral triangles. Again, the wave equation is considered and a grid refinement is performed. In this case the domain as well as the cells are equilateral triangles and the grid convergence corroborates second-order accuracy. (See Fig. 6.)
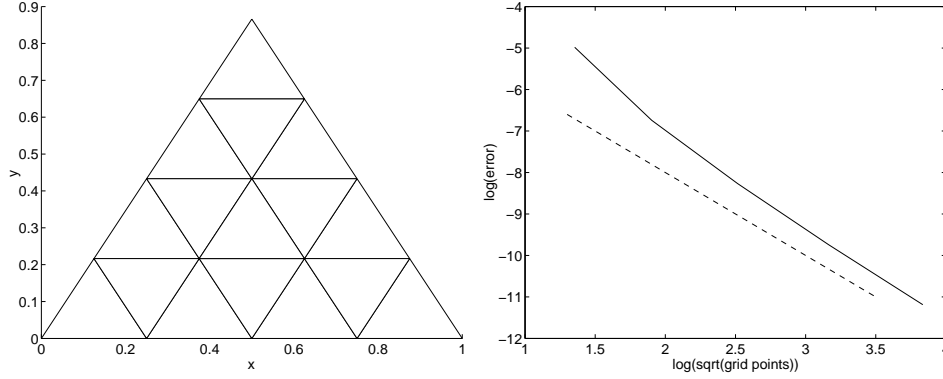
7

Figure 6: *Left:* A mesh with equilateral triangles. *Right:* Convergence for the wave equation with mesh consisting of equilateral triangles. The reference line represents second-order of accuracy.

It has been shown that the scheme works satisfactory on Cartesian as well as equilateral triangular grids which are both equilateral polygons. In fact, the scheme will work on grids consisting of any type of equilateral polygons. In the case of equilateral triangles the domain was also chosen to be a triangle. It is not possible to alter the shape of the cell triangles near the boundary since that would introduce errors of order 1.

The triangulated Cartesian grid used in Fig. 5 resulted in an inconsistent scheme. In the equilateral triangular case the scheme coincides with a mass lumped finite element scheme. To show the differences between finite volume and finite element schemes we derive the mass lumped finite element approximation of Laplace equation, with linear basis functions applied to the grid in Fig. 5 and obtain,

$$h^2(u_1)_t = -v_4 - v_3 + 4u_1 - u_7 - u_6.$$

The left hand side, $h^2(u_1)_t$, is the result of the mass lumping and is precisely equal to $V_1(u_1)_t$ obtained with the finite volume technique. However, the right hand side coincides with the ordinary finite difference scheme on the corresponding Cartesian grid. Compared to the finite volume case, different weights on all the neighbouring points are obtained and especially the cross derivative contribution is cancelled since u_5 and u_2 do not enter the scheme.

Remark We use the wave equation in our numerical computations, since it is a less forgiving equation. However, also for the heat equation on a triangulated Cartesian grid, the convergence levels out (see Fig. 7).
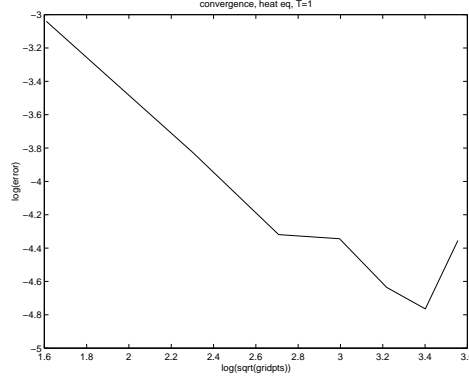
8

Figure 7: Convergence for the heat equation on a triangulated Cartesian grid.

3.2 A Different Finite Volume Approximation

To further explore the finite volume discretisations of viscous terms we will briefly discuss a discretisation proposed in [7] and also used in [6]. This discretisation allows for the computation of all viscous terms in the Navier-Stokes equations but it is not compact as the Laplace approximation previously discussed. The scheme is basically an application of the edge-based first derivative approximation (4) twice. In [7] it is observed that this scheme does not take into account the closest neighbours possibly yielding poor smoothing properties. (Compare the second derivative approximation that is obtained by applying a centred finite difference scheme twice.) Accordingly, they propose an augmented form that also uses the neighbours.

We will analyse consistency of the first derivative applied twice without this augmentation to see whether this can be used as an approximation of the Laplacian on more general grids. It certainly has the disadvantage that it is wider and thus not as computationally efficient. Recalling that N_i is the neighbours of the point indexed i and denoting by $(u_x)_i$ the approximation of the x-derivative at the same point we have that,

$$(u_x)_i = \frac{1}{V_i} \sum_{j \in N_i} \frac{u_j + u_i}{2} \Delta y_j, \tag{9}$$

where Δy_j is the difference (with sign) in the y direction going anti-clockwise along ds_{ij}. If approximation (9) is carried out for point 1 in Fig. 5, we would obtain with $V_1 = h^2$,

$$(u_x)_1 = \frac{1}{V_1} \sum_{j \in N_1} \frac{u_j + u_1}{2} \Delta y_j = u_x(x_1, y_1) + \mathcal{O}(h^2). \tag{10}$$

9

Further, if the grid in Fig. 5 is extended in all directions we obtain second order approximations similar to equation (10) of $(u_x)_i$ at all the points $2-7$.

Next, applying (9) for point 1 again, yields a first-order approximation of $(u_{xx})_i$.

$$(u_{xx})_1 = \frac{1}{V_1} \sum_{j \in N_1} \frac{(u_x)_j + (u_x)_1 + \mathcal{O}(h^2)}{2} \Delta y_j = u(x_1, y_1)_{xx} + \mathcal{O}(h) \qquad (11)$$

However, if the grid is not extended precisely as in Fig. 5, for example if the location of the points 2 and 5 are slightly disturbed or perhaps the diagonal between 1 and 5 is replaced by a diagonal between 4 and 6, a term of the form hu_{xy} will enter the Taylor expansion of (10). As an example, consider point 1 with the proposed diagonal altered. (Compare also to Fig. 4 where the orientaion of the diagonals are somewhat arbitrary.). Then,

$$(u_x)_1 = u_x(x_1, y_1) + const \cdot hu_{xy} + \mathcal{O}(h^2). \qquad (12)$$

Hence, we have shown that a first-order error may occur in the first derivative approximation. Then, suppose that $(u_x)_5$ has an error of the form (12). Then $(u_x)_i$, $i \in \{2, 3, 4, 6, 7\}$ in Fig. 5 are approximated to second-order and $(u_x)_5$ only to first-order. Applying (9) again to compute $(u_{xx})_1$ yields,

$$(u_{xx})_1 = \frac{1}{V_1} \sum_{j \in N_1} \frac{(u_x)_j + (u_x)_1 + \mathcal{O}(h)}{2} \Delta y_j = u(x_1, y_1)_{xx} + \mathcal{O}(1). \qquad (13)$$

Note that since $(u_x)_5 = u_x(x_5, y_5) + \mathcal{O}(h)$ is the only first order term there is no other term that can cancel that error. Multiplying by $\frac{\Delta y_5}{V_1} \sim \frac{1}{h}$, yields an error of $\mathcal{O}(1)$. This example shows that unless the grid has a high degree of regularity the scheme becomes inconsistent. The above considerations can be summarised in the following theorem.

Theorem 3.2 *On a general grid, the application of the first derivative approximation (9) twice to approximate a second derivative results in an inconsistent scheme.*

Remark Note that the above theorem does not imply that the scheme is inconsistent on all grids. As shown above, with certain restrictions imposed on the grid, the scheme is consistent.

As mentioned above, in [7] they propose an augmented form of the above approximation. However, the augmentation assumes implicitly that the above approximation is consistent. Thus, the same restriction of possible grids applies to their scheme as well.

4   The advection equation on mixed grids

We have already mentioned that the first derivative approximations do result in at least first-order accuracy on unstructured triangular grids (see [8] and Appendix I). However, as the previous section reveals, the finite volume approximations are not consistent on all grids, though they are assumed to be in real life computations. Hence, we go on studying a common technique used in CFD when constructing grids. That is to use structured Cartesian grids in boundary layers which is changed to triangular grids outside boundary layers which more easily adapts to complex geometries. Throughout, this section we will assume that $\epsilon = 0$ in equation (1).

4.1   Consistency analysis of interface

In this case we begin by analysing the first derivative approximation at an interface between unstructured triangles and quadrilaterals. In particular, we consider the finite volume approximation at an interface between arbitrary unstructured triangles triangular and a Cartesian grid. (See Fig. 8)
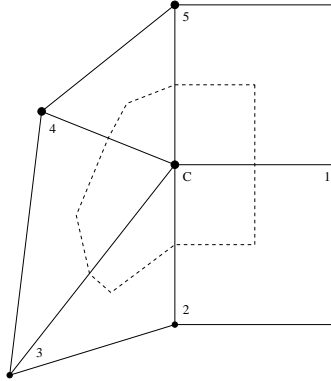

Figure 8: An interface between triangles and squares. The dashed line marks the dual grid.

We assume that the side of the squares have length h. This interface is smooth and we can derive the expected order of accuracy at the point c. The standard way of deriving order of accuracy is to make use of Taylor expansions. However, that becomes very complicated when unstructured triangles are considered. Instead, we will consider the two approximations obtained if the grid is split along the interface. Then we formally need to specify u_c on both sides using boundary conditions, but in this case u_c is given by the other side. First consider the finite volume approximation on

11

the control volume related to $1 - 2 - c - 5$. Denote the corresponding control volume V_c^C. (Note that the boundary of V_c^C partly coincides with $2 - c - 5$) The approximation (4) becomes,

$$V_c^C (u_c)_t = \frac{u_1 + u_c}{2} h + u_c(-h) \tag{14}$$

where c is a boundary point and the flux through the boundary is approximated by u_c. This is a consistent treatment of the boundary (see [8]) and the scheme is consistent.

The finite volume approximation (4) on the triangles becomes,

$$V_c^t (u_c)_t = \sum_{i=2}^{5} \frac{u_i + u_c}{2} \Delta y_i + u_c h, \tag{15}$$

where V_c^t is the corresponding control volume related to $c - 2 - 3 - 4 - 5$. (Again, it partly coincides with $2 - c - 5$ where it precisely matches V_c^C.) This is also a consistent approximation according to [8]. Note that, $V_c^t + V_c^C = V_c$. Hence, the sum of the two approximations is,

$$V_c (u_c)_x = \sum_{i=2}^{5} \frac{u_i + u_c}{2} \Delta y_i + \frac{u_1 + u_c}{2} h = \sum_{i=1}^{5} \frac{u_i + u_c}{2} \Delta y_i. \tag{16}$$

Note that, (16) is the same finite volume approximation at u_c as if the scheme had been applied directly ignoring the interface. Since it is constructed from two first-order approximations the sum is also at least first-order.

Since the finite volume approximation on a smooth quadrilaleral grid is also second-order accurate we conclude that the above reasoning applies to an interface between any smooth equilateral grid and triangles.

In order to derive the global order of accuracy we will use some theory from [8]. Consider the equation $u_t = u_x + F(x)$ with a finite volume discretisation $v_t = Dv + F$ where v denotes the vector with components v_i. D is the resulting matrix obtained by the finite volume discretisation, and F is a forcing function. According to [8] there is an energy estimate such that $\|v\| \leq constant(\|f\| + \|g\| + \|F\|)$ where f, g denotes the initial data and boundary data. $\|\cdot\|$ is the discrete l_2-norm (in two space dimensions) defined by,

$$\|a\|^2 = \sum_i a_i^2 V_i. \tag{17}$$

Then the error equation is,

$$e_t = De + T, \tag{18}$$

12

where $e = u - v$ and T is the truncation error. Note the e has zero initial and boundary data.

To derive the global order of accuracy we consider a hybrid grid with N^2 points in two space dimensions and a typical grid size $\mathcal{O}(h) = \mathcal{O}(1/N)$. The number of interface points is $\mathcal{O}(N)$ and $V_i \sim h^2$. Then from (18) we have $\|e\| \leq constant\|T\|$, i.e. the size of $\|e\|$ is proportional to the size of $\|T\|$. If we assume that the triangular grid is highly symmetric such that the local order of accuracy is 2 and the order of accuracy at the interface is 1 (as shown above) we obtain,

$$\|T\|^2 = \sum T_i^2 V_i \sim (\mathcal{O}(N)\mathcal{O}(h^2) + \mathcal{O}(N^2)\mathcal{O}(h^4))\mathcal{O}(h^2) = \mathcal{O}(h^3). \quad (19)$$

Hence $\|e\| \sim \|T\| \sim \mathcal{O}(h^{1.5})$, i.e. the order of accuracy is 1.5. (If the accuracy on the triangular part is only first order the global order order of accuracy will be 1.)
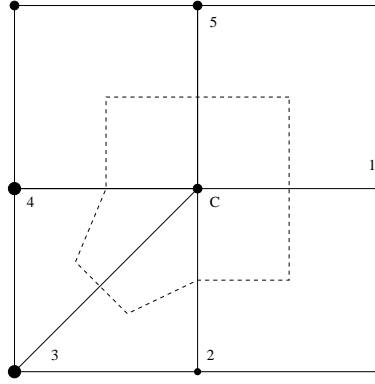
Next, consider the interface in Fig. 9.

Figure 9: An interface between triangles and squares. The dashed line marks the dual grid.

If we assume that a grid refinement would keep the corner we obtain from Taylor expansions with the sides of the squares have length h. Then $V_c = \frac{5}{6}h^2$

13

and,

$$u_1 = u_c + hu_x + \frac{h^2}{2}u_{xx} + \mathcal{O}(h^2),$$

$$u_2 = u_c - hu_y + \frac{h^2}{2}u_{yy} + \mathcal{O}(h^2),$$

$$u_3 = u_c - hu_x - hu_y + \frac{h^2}{2}(u_{yy} + u_{xx} + 2u_{xy}) + \mathcal{O}(h^2),$$

$$u_4 = u_c - hu_x + \frac{h^2}{2}u_{xx} + \mathcal{O}(h^2),$$

$$u_5 = u_c + hu_y + \frac{h^2}{2}u_{yy} + \mathcal{O}(h^2),$$

The finite volume approximation (4) becomes,

$$V_c u_t(x_c, y_c) = \frac{u_c + u_1}{2}h + \frac{u_c + u_2}{2}\frac{h}{6} + \frac{u_c + u_3}{2}\frac{(-h)}{3} + \frac{u_c + u_4}{2}\frac{(-5h)}{6} =$$

$$V_c u_x(x_c, y_c) + \frac{h^2}{12}u_y(x_c, y_c) + \mathcal{O}(h^3). \, (20)$$

Shifting the diagonal in Fig. 9 will not improve things. In either case, we have an $\mathcal{O}(1)$ error at c.

If we assume that we have an interface with a number of corners like the one above. With two space dimensions and a total number of points $\mathcal{O}(N^2)$ there are $\mathcal{O}(N)$ corner points with an $\mathcal{O}(1)$ error. Again,we consider the error equation and use the energy estimate derived in [8] to conclude that $\|e\| \sim \|T\|$. To determine the size of the truncation error, assume that the order of accuracy away from corners is 1, i.e $T_i \sim \mathcal{O}(h) = \mathcal{O}(1/N)$ at those points.

$$\|T\|^2 = \sum_i T_i^2 h^2 \sim \mathcal{O}(h^2)(\mathcal{O}(N)\mathcal{O}(1)^2 + \mathcal{O}(N^2)\mathcal{O}(1/N)^2) = \mathcal{O}(h). \quad (21)$$

Then $\|T\| \sim \mathcal{O}(h^{1/2}) \sim e$, i.e the order of accuracy is 0.5.

Theorem 4.1 *Consider a hybrid mesh composed of unstructured triangles and smooth quadrilaterals with a non-smooth interface. Then the approximation (4) of (1) with $b = \epsilon = 0$ is inconsistent at the interface and the global order of accuracy reduces to 0.5.*

Note that throughout this article we consider a model problem with two space dimensions and we assume implicitly in Theorem 4.1 that an interface is one-dimensional. In general we consider an interface to be a $d-1$ surface in

14

q	N_{tot}	q_i	N_b	q_tot	interface type
2	N^2	1	N	1.5	smooth,2D
1	N^2	1	N	1	smooth,2D
2	N^2	0	N	0.5	non-smooth,line,2D
2	N^2	0	1	1	non-smooth,point,2D
2	N^3	1	N^2	1.5	smooth,3D
1	N^3	1	N^2	1	smooth,3D
2	N^3	0	N^2	0.5	non-smooth,plane,3D
2	N^3	0	N	1	non-smooth,line,3D
2	N^3	0	1	1.5	non-smooth,point,3D

Table 1: Order of accuracy for hybrid meshes. q is the lowest order of accuracy of the scheme away from the interface. N_{tot} is the total number of points. (We assume N points in one space dimension.) q_i is the order of accuracy at interface points. (0 meaning order 1 error.) N_b is the number of boundary points. q_{tot} is the resulting overall order of accuracy.

a problem with d space dimensions. One can anticipate even more restrictive constraints in higher-dimensional problems. If there is a disconituity at one or many points or even along a subsapce of the interface order 1 errors will be introduced. With the the same technique as used above to estimate the l_2-norm of the truncation error we get the results displayed in Table 1 in two and three space dimensions.

4.2   Computations

Consider, equation (1) with $a = 1, b = 1$ and $\epsilon = 0$ on a two-dimensional rectangular domain discretised by (4). The initial data is $u(x, 0) = a sin(4\pi(ax + by))$ and the exact solution, $u(x, t) = sin(4\pi(a(x - t) + b(y - t)))$. The exact solution is also used as boundary data.

In Fig. 10 the convergence rate for a triangular grid is displayed. The convergence rate is close to 2 which is due to the fact that the grid is very symmetric.
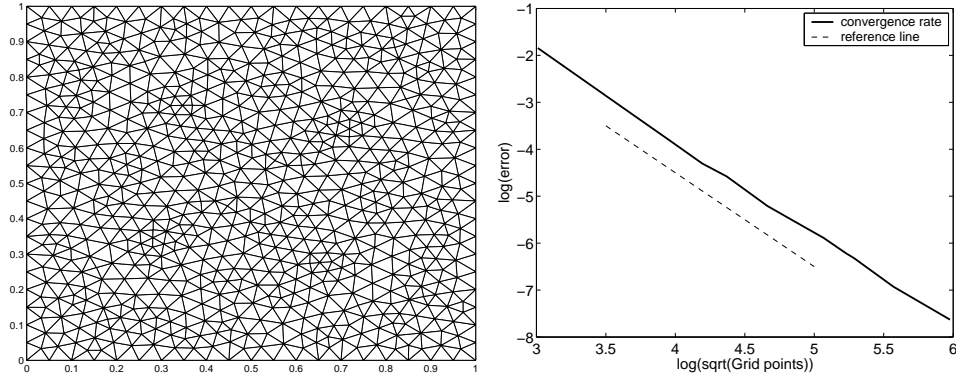
Figure 10: *Left:* A triangular mesh with 727 grid points. *Right:* Convergence rate for the advection equation on triangular meshes. The dashed reference line represents second-order of accuracy.

We also consider a quadrilateral grid (see Figure 11) where there is a smooth mapping to a Cartesian grid. In this case we also obtain second-order accuracy. See Table 2
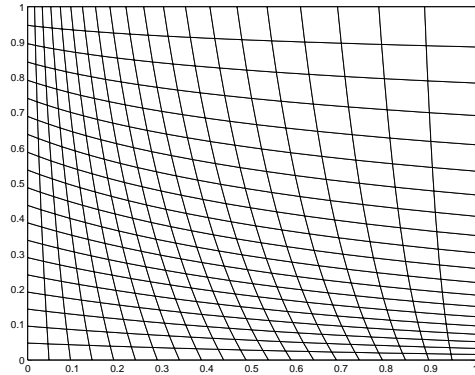

Figure 11: A smooth quadrilateral grid.

To illustrate that the smoothness is essential for quadrilateral grids we show the convergence properties for quadrilateral grids (without stretching) with a 20% perturbation in the x- and y-direction for each node. This yields a sequence of non-smooth quadrilateral grids. (See Figure 12).

16

$\sqrt{N}$	l_2-error	l_2-convergence	$l_\infty - error$
41	0.0325	-	0.2497
81	0.0080	2.06	0.1054
121	0.0035	2.06	0.0415
161	0.0020	1.98	0.02195
201	0.0013	1.92	0.0152
241	9.05e-4	2.00	0.0107
281	6.76e-4	1.90	0.0075

Table 2: Errors and convergence on smooth quadrilateral grids.

$\sqrt{N}$	l_2-error	l_2-convergence	$l_\infty - error$
41	0.0424	-	0.1187
81	0.0225	0.93	0.1243
121	0.0192	0.40	0.1393
161	0.0179	0.25	0.1534
201	0.0168	0.29	0.1551
241	0.0161	0.23	0.1382
281	0.0160	0.04	0.1855

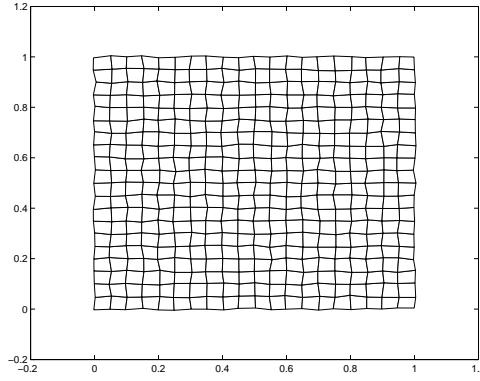Table 3: Errors and convergence on non-smooth quadrilateral grids.

Figure 12: A non-smooth quadrilateral grid.

In Table 3 it is seen that there is no convergence in l_∞ and in l_2 the convergence drops towards 0. The results in l_∞ shows that there are $\mathcal{O}(1)$ errors present at at least one point. Since the l_2-error does not go to zero we conclude that the number of inconsistent points are proportional to the total number of points. This is what we would expect since there are perturbations

17

$\sqrt{N}$	l_2-error	l_2-convergence	$l_\infty - error$
41	0.0352	-	0.2603
81	0.0087	2.05	0.1035
121	0.0038	2.06	0.0412
161	0.0022	1.91	0.0353
201	0.0014	2.04	0.0291
241	0.0010	1.85	0.0246
281	7.5e-4	1.87	0.0218

Table 4: Hybrid quadrilateral and triangular grid with smooth interface.

to the nodes everywhere.

Next, we turn to mixed grids. We begin our study with the same smooth quadrilateral grid used above. The total number of points is $(N+1)^2$ and we place an interface at $x(N/2+1)$. This yields a smooth interface. On one side we triangulate the grid and on the other we keep the quadrilaterals (See Figure 13). According to the previous theory this should have order of accuacy 1.5. The errors and convergence are displayed in Table 4 and we see that the errors in l_2 and l_∞ are convergent.
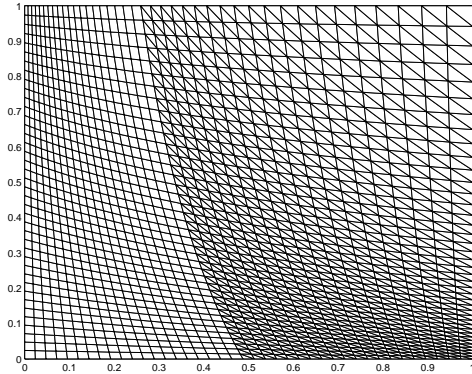

Figure 13: A hybrid quadrilateral and triangular grid with a smooth interface.

However, as previously mentioned, it is common that the interface is non-smooth. (See Figure 1.) An example of such an interface is displayed in Figure 14 and the convergence data given in Table 5.

$\sqrt{N}$	l_2-error	l_2-convergence	$l_\infty - error$
41	0.0338	-	0.1329
81	0.0144	1.23	0.1015
121	0.0108	0.72	0.1003
161	0.0091	0.60	0.0999
201	0.0081	0.52	0.1004
241	0.0074	0.50	0.1006
281	0.0068	0.55	0.1004
321	0.0064	0.46	0.1004

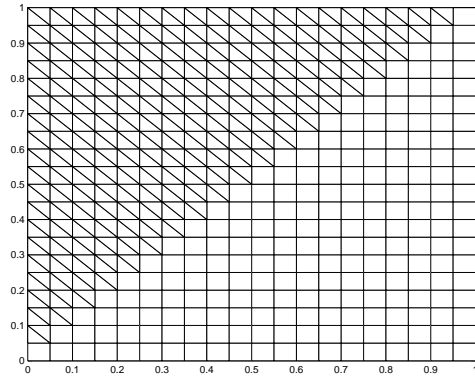Table 5: Hybrid quadrilateral and triangular grid with non-smooth interface.

Figure 14: A hybrid quadrilateral and triangular grid with a non-smooth interface.

Clearly, there are points that are non-convergent according to Table 5. As shown above the l_2-convergence should approach 0.5 which is corroborated in Table 5.

5 Conclusions

Edge-based node-centred finite volume approximations are widely used in computational aerodynamics for one important reason. They are assumed accurate on unstructured grids.

In Theorem 3.1 and 3.2, we prove that discretisations of second derivatives with two different commonly used approximations are inconsistent on unstructured grids. However, the accuracy is recovered on grids with a high level of regularity. For the Laplacian approximation equilateral polygons

are required and for the first derivative approximation applied twice slightly more general grids can be allowed.

The CFD community (see for example [18]) have recognised that in boundary layers, Cartesian grids should be used in order to obtain better accuracy (see Fig 1). Our analysis confirm that observation since the viscous terms are dominant in the boundary layer and those are only approximated correctly on regular grids, such as rectangles and equilateral polygons.

Structured grids in boundary layers and unstructured to capture geometries have led us to study mixed grids for the first derivative approximation. That approximation is shown to be consistent on triangular grids and on smooth quadrilateral grids. For mixed grids with smooth interfaces between the quadrilaterals and triangles the accuracy is not degraded.

However, if the interface is non-smooth the order of accuracy drops to 0.5 due to inconsistencies in the discretisation. To summarise, care has to be taken when constructing hybrid grids. Extensive numerical experiments corroborate our theoretical results.

APPENDIX

I   First derivative approximation

We will show that the first derivative approximation is first order accurate on a general triangular grid. This derivation is due to [19].
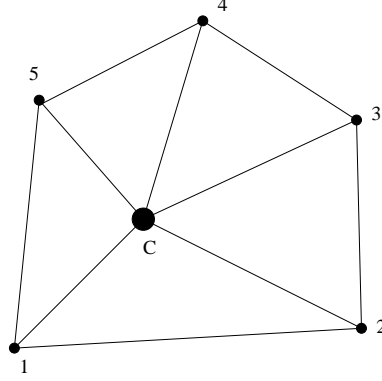
Consider the grid in Fig. 15.

Figure 15: A general triangular grid.

The approximation of u_x at the centre point c is,

$$(u_x)_c = \frac{1}{V_c} \sum_i \frac{u_c + u_i}{2} \Delta y_i, \qquad (22)$$

where V is the volume the measure of the volume of the dual grid. If this approximation is first order accurate it should exactly differentiate a constant and a linear function.

For a constant function $u = C$ we have $u_x = 0$ and,

$$(u_x)_c = \frac{C}{V} \sum_i \Delta y_i = 0. \qquad (23)$$

Hence, the approximation is correct for a constant. Next, we turn to a linear function $u = ax + by$ where a and b are constants and $u_x = a$. Denote by $\tilde{r}_1 = (\tilde{x}_1, \tilde{y}_1)$ the position of the centre of mass for the triangle $1, 2, c$ and $\tilde{r}_2$ for the triangle $2, 3, c$ etc. Then the approximation for the linear function is,

$$(u_x)_c = \frac{1}{V_c} \sum_{i=1}^{max} \frac{ax_c + by_c + ax_i + by_i}{2} (\tilde{y}_i - \tilde{y}_{i-1}) =$$

$$\frac{1}{V} \sum_{i=1}^{max} \frac{ax_i + by_i}{2} (\tilde{y}_i - \tilde{y}_{i-1}), \qquad (24)$$

21

where $\tilde{y}_0$ is interpreted as $\tilde{y}_{max}$ in a cyclic manner around c. (In Fig 15 $max = 5$.) Hence, it is always assumed assumed that we compute *modulo* the number of neighbours.

The y-coordinate of the centre of mass is obtained by,

$$\tilde{y}_i = \frac{y_i + y_{i+1} + y_c}{3}.$$ (25)

Then,

$$\tilde{y}_i - \tilde{y}_{i-1} = \frac{y_i + y_{i+1} + y_c}{3} - \frac{y_i + y_{i+1} + y_c}{3} = \frac{y_{i+1} - y_{i-1}}{3}.$$ (26)

Using (26) in (24) results in,

$$(u_x)_c = \frac{1}{V_c} \sum_i \frac{ax_i}{2} \frac{y_{i+1} - y_{i-1}}{3} + \frac{by_i}{2} \frac{y_{i+1} - y_{i-1}}{3}.$$

Note that,

$$\sum_{i=1}^{max} y_i (y_{i+1} - y_{i-1}) = 0.$$

Hence,

$$(u_x)_c = \frac{a}{V_c} \sum_i x_i \frac{y_{i+1} - y_{i-1}}{6}.$$ (27)

Next, we will compute V_c. The triangle $1, 2, c$ has the area,

$$\frac{1}{2} |(r_1 - r_c) \times (r_2 - r_c)|$$

where $r_i = (x_i, y_i)$ is the point vector at point i. With the same notation as for $\tilde{r}_i$ we denote the area of traingle $i, i+1, c$ by A_i. Hence,

$$A_i = \frac{1}{2}((x_i - x_c)(y_{i+1} - y_c) - (y_i - y_c)(x_{i+1} - x_c)).$$

The area of the dual volume is,

$$V_i = \sum_i \frac{1}{3} A_i = \sum_i \frac{1}{6}((x_i - x_c)(y_{i+1} - y_c) - (y_i - y_c)(x_{i+1} - x_c)) =$$

$$\frac{1}{6} \sum_i x_i y_{i+1} - x_i y_c - x_c y_{i+1} + x_c y_c - (y_i x_{i+1} - y_c x_{i+1} - y_i x_c + y_c x_c) =$$

$$\frac{1}{6} \sum_i x_i y_{i+1} - y_i x_{i+1} = \frac{1}{6} \sum_i x_i (y_{i+1} - y_{i-1})$$ (28)

22

Note that we use modulo calculations extensively which also justifies the shift of the indices. With (28) in (27) we have,

$$(u_x)_c = a.$$

Hence, we have shown first order accuracy on an arbitrary triangular grid.

References

[1] A. Haselbacher, J.J. McGuirk, and G.J. Page. Finite volume discretization aspects for viscous flows on mixed unstructured grids. *AIAA Journal*, 37(2), Feb. 1999.

[2] D.J Mavriplis. Accurate multigrid solution of the Euler equations on unstructured and adaptive meshes. *AIAA Journal*, 28(2), Feb. 1990.

[3] D.J Mavriplis. Multigrid strategies for viscous flow solvers on anisotropic unstructured meshes. *J. Comput. Physics*, 145, 1998.

[4] D.J. Mavriplis and D.W. Levy. Transonic drag prediction using an unstructured multigrid solver. Technical report, Institute for Computer Applications in Science and Engineering, 2002.

[5] D.J. Mavriplis and V. Venkatakrishnan. A unified multigrid solver for the Navier-Stokes equations on mixed element meshes. Technical report, Institute for Computer Applications in Science and Engineering, 1995.

[6] T. Gerhold, O. Friedrich, and J.Evans. Calculation of complex three-dimensional configurations employing the *DLR-τ-Code*. In *AIAA paper 97-0167*, 1997.

[7] J.M. Weiss, J.P. Maruszewski, and W.A. Smith. Implicit solution of preconditioned Navier-Stokes equations using algebraic multigrid. *AIAA Journal*, 37(1), Jan. 1999.

[8] Jan Nordström, Karl Forsberg, Carl Adamsson, and Peter Eliasson. Finite volume methods, unstructured meshes and strict stability for hyperbolic problems. *Applied Numerical Mathematics*, 45(4), June 2003.

[9] M. Svärd and J. Nordström. Stability of finite volume approximations for the laplacian operator on quadrilateral and triangular grids. *Applied Numerical Mathematics*, 51(1), October 2004.

[10] W.K. Anderson and D.L. Bonhaus. An implicit upwind algorithm for computing turbulent flows on unstruxtured grids. *Computers and Fluids*, 23(1), January 1994.

[11] E.J. Nielsen and W.K. Anderson. Recent improvements in aerodynamic design optimization on unstructured meshes. In *AIAA-2001-0596*, 2001.

[12] E.J. Nielsen, J. Lu, M. Park, and D.L. Darmofal. An implicit, exact dual adjoint solution method fo turbulent flows on unstructured grids. *Computers and fluids*, 33, 2004.

[13] Y. Kallinderis. A 3-D finite-volume method for the Navier-Stoekes equations with adaptive hybrid grids. *Applied Numerical Mathematics*, 20, 1996.

[14] Lars Tysell. Hybrid grid generation for complex 3d geometries. In *Proceedings of 7th International Conference on Numerical Grid Generation in Computational Field Simulation, Whistler,British Columbia,Canada*, pages 337–346, 2000.

[15] D. Kim and H. Choi. A second-order time-accurate finite volume method for unsteady incompressible flow on hybrid unstructured grids. *Journal of Computational Physics*, 162, 2000.

[16] R.P. Koomullil, D.S. Thompson, and B.K. Soni. Iced airfoil simulation using generalized grids. *Applied Numerical Mathematics*, 46, 2003.

[17] J. Gong, M. Svärd, and J. Nordström. Artificial dissipation for strictly stable finite volume methods on unstructured meshes. In *WCCM VI in conjuction with APCOM'04, Beijing, China*, 2004.

[18] D.J Mavriplis. Unstructured grid techniques. *Annu. Rev. Fliud. Mech.*, 29, 1997.

[19] Karl Forsberg. The Swedish Defence Research Agency. Private Communication.

REPORT DOCUMENTATION PAGE

The public reporting burden for this collection of information is estimated to average 1 hour per response, including the time for reviewing instructions, searching existing data sources, gathering and maintaining the data needed, and completing and reviewing the collection of information. Send comments regarding this burden estimate or any other aspect of this collection of information, including suggestions for reducing this burden, to Department of Defense, Washington Headquarters Services, Directorate for Information Operations and Reports (0704-0188), 1215 Jefferson Davis Highway, Suite 1204, Arlington, VA 22202-4302. Respondents should be aware that notwithstanding any other provision of law, no person shall be subject to any penalty for failing to comply with a collection of information if it does not display a currently valid OMB control number.
PLEASE DO NOT RETURN YOUR FORM TO THE ABOVE ADDRESS.

1. REPORT DATE *(DD-MM-YYYY)*	2. REPORT TYPE	3. DATES COVERED *(From - To)*

4. TITLE AND SUBTITLE	5a. CONTRACT NUMBER
	5b. GRANT NUMBER
	5c. PROGRAM ELEMENT NUMBER
6. AUTHOR(S)	5d. PROJECT NUMBER
	5e. TASK NUMBER
	5f. WORK UNIT NUMBER

7. PERFORMING ORGANIZATION NAME(S) AND ADDRESS(ES)	8. PERFORMING ORGANIZATION REPORT NUMBER

9. SPONSORING/MONITORING AGENCY NAME(S) AND ADDRESS(ES)	10. SPONSORING/MONITOR'S ACRONYM(S)
	11. SPONSORING/MONITORING REPORT NUMBER

12. DISTRIBUTION/AVAILABILITY STATEMENT

13. SUPPLEMENTARY NOTES

14. ABSTRACT

15. SUBJECT TERMS

16. SECURITY CLASSIFICATION OF:			17. LIMITATION OF ABSTRACT	18. NUMBER OF PAGES	19b. NAME OF RESPONSIBLE PERSON
a. REPORT	b. ABSTRACT	c. THIS PAGE			19b. TELEPHONE NUMBER *(Include area code)*